THE BALTIC JOURNAL
OF ROAD AND BRIDGE ENGINEERING

2012
7(2): 104–111

INFLUENCE OF CRACKING ON DEFLECTIONS OF CONCRETE BOX GIRDER BRIDGES

Chao Liu[1]✉, Dong Xu[2]

Dept of Bridge Engineering, Tongji University, Siping Rd.1239 Shanghai, 200092, China
E-mails: [1]lctj@tongji.edu.cn; [2]xu_dong@tongji.edu.cn

Abstract. The problem of cracking and long-term deflection in larger-span prestressed concrete box girder bridges exists throughout the world and has restricted the development of long-span concrete bridges to some extent. However, the understanding of cracking and deflection of concrete box girder bridges is still insufficient and many strengthening methods cannot reach anticipated effect. In this paper, a space-frame lattice model which is used to analyze the stress on the entire cross-section of the box girder bridge, is presented. The stress state of random grid elements in the model may be biaxial in plane. The model simulates the cracking and deflection of pre-stressed concrete box girder bridges. This model was applied for cracking and deflection analysis of the existing concrete box girder bridge with (80+100+80) m spans. The calculation results are compared with the actual status of the bridge. The paper indicates that cracking of girder becomes one of major factors which have influence on deflections of long span prestressed concrete bridges. The space-frame lattice model is an effective tool to analyze the cracking and deflection of prestressed concrete box girder bridges and merits further investigation.

Keywords: concrete box girder bridge, space frame lattice model, bottom slab cracking, web cracking, deflection, shear stress, principle tensile stress.

1. Introduction

The box girder with a closed cross-section, which has better global behaviour, larger torsion stiffness and an effective top and bottom concrete flange in compression, is widely used in large bridge structures. In particular, the prestressed concrete box girder bridges, which are suitable for various modern construction methods, have superior applicability. The prestressed concrete beam bridges also have greater economy in larger-span bridge structures. Since the 1970's, prestressed concrete box girder bridges have been predominately applied in the design of bridges with medium- and long-spans. Up to now, more than 20 continuous rigid frame bridges with the span larger than 200 m and more than 100 prestressed concrete continuous girder bridges with the span between 100 and 200 m have been built or are under construction. There are about 18 super-span continuous rigid frame bridges with the span larger than 240 m in the world, 13 of which are located in China. This amounts to more than 70% of the total and it is still increasing (Xu 2008).

However, since many of the long-span prestressed concrete box girder bridges have been built more and more defects appeared. Box girder cracking and long-term deflection of the mid-span may be the most serious problems (Krístek *et al.* 2006; Krístek, Kohoutková 2006; Lou 2006; Robertson 2005). For example, in Huangshi Yangtze River Bridge in China, completed in 1995, a crack width of 0.4 mm was found and long-term mid-span deflection with a max of 335 mm during the investigation in 1998 (Xie *et al.* 2007). For the secondary navigation channel of Humen Bridge, the actually measured mid-span deflection was 260 mm seven years after completion (Qi *et al.* 2007). The mid-span deflection of the Stolma Bridge in Norway, with main span 301 m, was 92 mm three years after completion (Xie *et al.* 2007). The bridges mentioned above are all prestressed concrete continuous beam bridges. The best representative, the Koror-Babeldaob Bridge in Palau with the main span of 241 m, completed in 1977, was the longest prestressed concrete girder bridge in the world at that time. By 1990, the sag of the centre line had reached 1.2 m, affecting the appearance of the bridge, causing discomfort to the passersby and damage to the pavement. A strengthening method proposed by VSL International was carried out by Black Micro (a local firm) in 1995. The remedial work was completed in July 1996. Unexpectedly, three months after strengthening, the bridge suddenly collapsed catastrophically into the river (Burgoyne, Scantlebury 2006).

Based on the initial statistical analysis, the relationship between the annual average rate of deflection (*f*) and

ISSN 1822-427X print / ISSN 1822-4288 online
doi: 10.3846/bjrbe.2012.15
http://www.bjrbe.vgtu.lt

the length of the main span (L) of long-span prestressed concrete beam bridges is as following (Xu 2008):

L = 100~160 m, f = 5~10 (mm/year);

L = 160~220 m, f = 10~20 (mm/year);

L = 220~270 m, f = 20~30 (mm/year).

It is noteworthy that the cracking and deflection of structures are usually interactive.

Therefore, the problem of cracking and long-term deflection in larger-span prestressed concrete box girder bridges exists throughout the world and has restricted the development of long-span concrete bridges to some extent. However, the understanding of cracking and deflection of box girder bridges is still insufficient and many strengthening methods cannot reach anticipated effect. There are many reasons for the change in deflection which are usually coupled together (Barr, Angomas 2010; Gwoździewicz *et al.* 2000; Hu 2005; Huang *et al.* 2009; Liu *et al.* 2008; Rodriguez 2004; Qi *et al.* 2007; Shao *et al.* 2011; Števula, Vitek 1998; Zheng *et al.* 2011): (1) the realistic prediction of concrete creep and shrinkage; (2) the efficiency of prestressing to reduce deflections; (3) the shear deformations and the shear lag; (4) concrete cracking, and so on. More attention has been paid to the first three factors by engineers. Research shows that there are about 15% of the errors in different mathematical models for creep and shrinkage but this error is always convergent (Xie *et al.* 2007). That is to say, whatever the error of the mathematical models is, the phenomenon of long-term sagging of structure caused by creep does not happen.

The authors believe that under the condition that the quality of construction and materials matches the corresponding standards the primary influence on long-term deflection would be caused by cracking of the structure.

2. Stress characteristics of box girder cross-section

The internal force state of a spatial bridge structure is expresed by six forces: the axial force N, the shear force along vertical and transverse directions Q_x and Q_y, the flexural moment along transverse and longitudinal directions M_x and M_y, and the torsion moment M_z (Du 1994; Xiang 2001). The six forces in box section are combined and decomposed in terms of stress, as shown in Fig. 1 (Xu 2008). The normal stress is produced by axial force N and flexural moment M_x (M_y), while the shear stress is produced by shear force Q_x (Q_y) and torsion moment M_z, and these stresses are superimposed on each other. Thus, six forces are merged to normal stress and shear stress. Because the principal stress is composed of normal stress and shear stress, the stress characteristics of box girder cross-section is judged by principal stress.

The cross-section of bridge structure is composed by structural "plate" member with two-dimensional (2D) stress. The difference between one-dimensional (1D) stress and 2D stress is as following: the crack generated by 1D stress begins from the edge of cross-section and not penetrates to the plate along thickness, and the shear stress is transferred, while the crack generated by 2D stress penetrates to the plate along thickness, and the shear stress is not transferred.

For the box girder bridges, the 2D stress (principal stress) in the middle layer of top and bottom flange of box girder is often ignored in design, as shown in Fig. 2. For example, the principal tensile stress at D in Fig. 2 is in horizontal plane and the vertical prestressing not influences the stress at D. The shear stress (principal tensile stress) here is reduced only through optimizing the longitudinal prestressed tendons, which reduces the flexural shear flow of bottom slab by reducing the shear of box girder cross-section. But with the development of the bigger prestressed strands, the anchoring force is so large that generates big stress concentration in anchor block. Because of the anchoring of internal prestressed tendons in bottom slab, the bigger horizontal shear in plane of bottom slab will be generated and it combines with the flexural shear flow in bottom slab. If the combined principal tensile stress exceeds the actual concrete ultimate tensile stress, inclined cracking will occur in the plane of bottom slab. If constructional reinforcements in bottom slab are insufficient, steel will yield and move among the concrete, and then influence the longitudinal stress and deformation of the box girder significantly (Liu *et al.* 2010). Once the above situation occurs, the bottom slab will crack and the shear stress in the web will increase because the closed cross-section of box girder will change into an open cross-section with concrete cracking. The above mentioned condition was analyzed by theoretical calculations (Zhang 2007) and it was concluded that the max shear stress in the web would increase by 15~20% after bottom slab cracking. In addition, the effect of longitudinal prestressing in the bottom

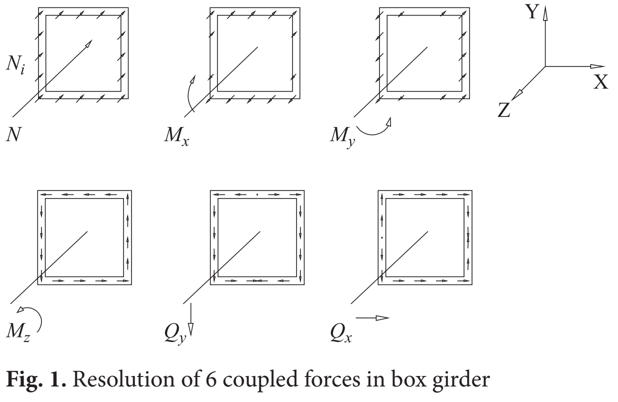

Fig. 1. Resolution of 6 coupled forces in box girder

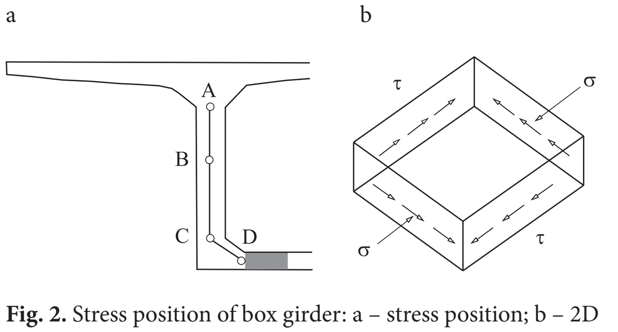

Fig. 2. Stress position of box girder: a – stress position; b – 2D stress in plane at D (τ – shear stress, σ – normal stress)

slab is not accurately transferred to the web, and then the cracking in web will occur because the principal tensile stress of web is too large.

3. Space-frame lattice model

There is a detailed introduction about space frame lattice model (Liu *et al.* 2010). For example, a box girder is separated into the top slab, bottom slab and many webs, as shown in Fig. 3. This model is like the up-stand finite element modelling presented by Eugene J. O'Brien and Damien L. Keogh (Keogh *et al.* 1996; O'Brien, Keogh 1998, 1999). They presented a plate finite element model for a cellular bridge deck in 1999. Unfortunately at that time, the number of elements required to achieve correct results was very large and this, combined with the tedium of interpreting the results, often ruled out its use. Recently, computer technology and calculation software have already developed into a new period and the application of this kind of model totally comes true (Grigorjeva *et al.* 2008; Kaklauskas *et al.* 2008; Liu *et al.* 2010; Xu 2008). Thus, the space-frame lattice model for the analysis of concrete box girder cracking and deflection is presented.

Fig. 4 shows a space-frame lattice model for a prestressed concrete box girder bridge with a single-cell at the third cantilever construction state. Fig. 5 shows a space-frame lattice model for a steel-concrete composite cable-stayed bridge with twin main girders. Space-frame lattice model, as well as dealing with a varying neutral axis, has the advantage of automatically allowing for transverse cell distortion. Transverse diaphragms could also be incorporated into this model with ease. When using this model, the equivalent loading due to prestress is applied in a three-dimensional (3D) manner. Many of the complications involved in determining equivalent loads due to prestress are avoided in this way. There is no uncertainty concerning the location of the neutral axis about which eccentricity of prestress must be calculated. There are also advantages to be gained in the interpretation of results, because they are related directly to the design unnecessary to distinguish primary and secondary effects. This method is often simpler to implement as it is unnecessary to uncouple the in-plane and out-of-plane behaviours. The model simulates the stress in every part of bridges according to the engineers because it takes into account all the spatial effects except for Poisson's ratio.

In the calculation model of the box girder structure expressed by the space-frame lattice the longitudinal effect (axial force and flexural moment) is carried by the longitudinal grid while the transverse effect (frame effect and distortion) is carried by the transverse grid. The effect of torsion and distortion of the box girder cross-section is converted into shear differences in the web grid, and the

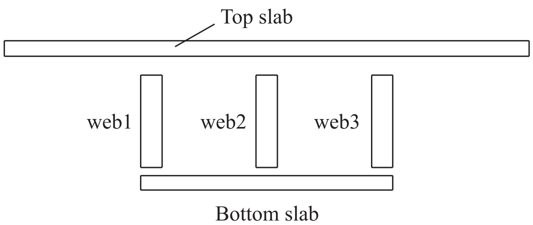

Fig. 3. A double-cell box section expressed by "plates"

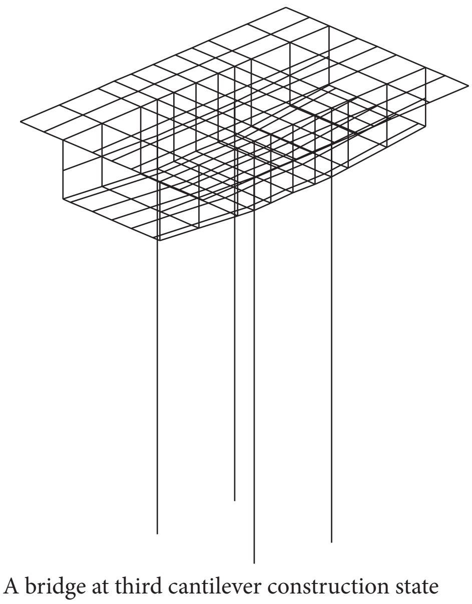

Fig. 4. A bridge at third cantilever construction state

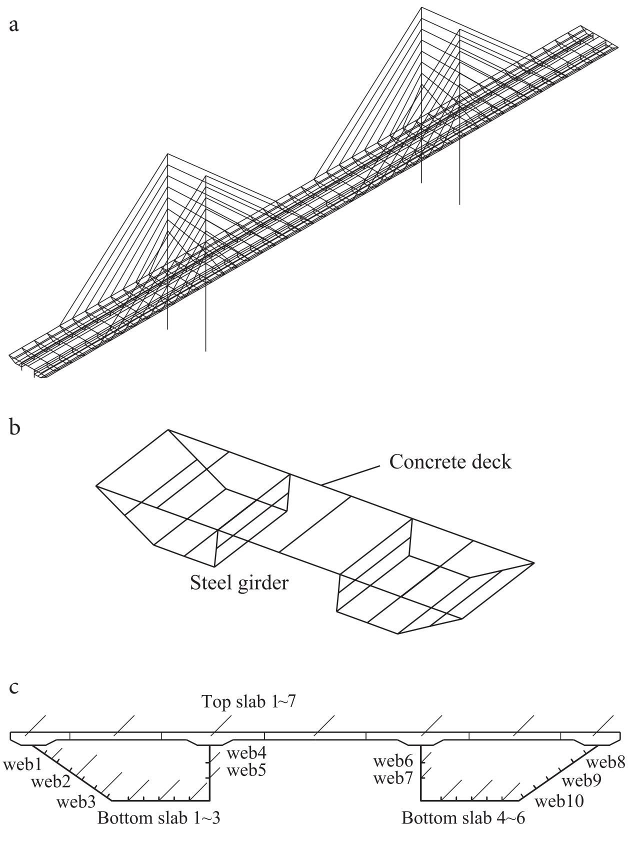

Fig. 5. Space-frame lattice model of steel-concrete composite cable-stayed bridge with twin main girder: a – space-frame lattice model of the whole bridge; b – a segment; c – section divided

shear lag effect of the top and bottom slab of the box girder cross-section is expressed by different forces of different longitudinal grid elements. The final calculation results are expressed by the force of longitudinal and transverse grids.

The space-frame lattice model, the output results of which are more meticulous and numerous than the ones expressed by the single beam model, is suitable for analysis on stress of the entire cross-section. The stress state of random grid elements in the model may be biaxial in plane (Fig. 2). The box girder cracking is determined by analyzing the stress state of grid elements at the space-frame lattice model and simulated by partially removing the element or modifying the rigidity of the element at the cracked region, and then the numerical simulation process is repeated to find the final behaviours of the structure.

4. Calculation example of a bridge with cracking and deflection

4.1. Introduction

To try to find the influence of cracking on the deflection of a structure an actual bridge with cracking and deflection was simulated and analyzed by the space-frame lattice model. This bridge is a prestressed concrete continuous box girder bridge with (80+100+80) m spans, completed in 1995. The main girder with single box and single cell is shown in Fig. 6, and longitudinal profile of bridge is shown in Fig. 7. The height of box girder at pier is 5.8 m, while the height of box girder at the mid-span and the end of side span is 2.4 m which changes by quadratic parabola. The bridge contains the whole internal prestressing system, i.e., tri-directional prestressing system in longitudinal, transverse and vertical directions (Fig. 8).

The situation of this bridge, detected in 2007, is as following:

Table 1. Situation of the bridge

Item	Situation
1	The inclined cracks in the box girder webs were numerous within 5 m of both side-span supports. The most lengths of cracks were between 0.15~0.25 m, and the max width reached 0.5 mm.
2	Many parallel cracks in the longitudinal direction of the bridge existed along the bottom slab of the box girder at mid-span of both side-spans. The most widths of cracks were 0.1 mm and the max width reached 0.25 mm. The spaces between cracks were 15~40 cm.
3	The max downward deflection of the girder in the side span was about 5.4 cm, while the max upward deflection of the girder at mid-span was about 7 cm.

The photos of inclined cracks in the web and longitudinal cracks in the bottom slab are shown in Fig. 9.

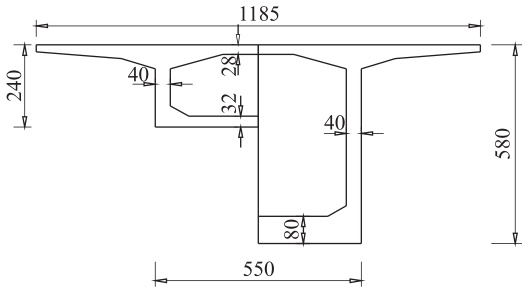

Fig. 6. Box girder section in cm

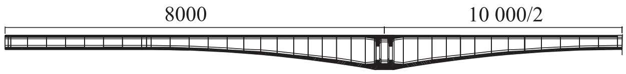

Fig. 7. Longitudinal profile of half bridge in cm

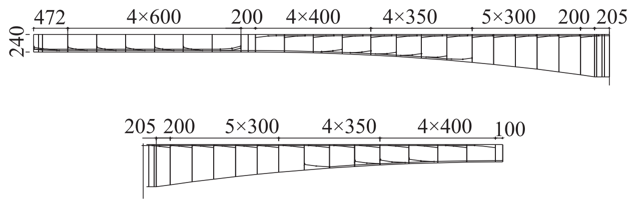

Fig. 8. Layout of the prestressing system of half bridge in cm

a b

Fig. 9. Cracks: a – inclined cracks in web; b – longitudinal cracks in bottom slab (from Wang J.) (Xu 2008)

4.2. Calculation model

The space-frame lattice model of the half bridge is shown in Fig. 10. The top slab of the box girder is divided into 11 longitudinal grids, while the bottom slab is divided into 5 longitudinal grids. For the layout of internal prestressed tendons the web is divided into one longitudinal grid only. The division of the cross-section is shown in Fig. 11.

The calculation was carried out according to the true construction stages of this bridge, the influence of 12 years creeping is considered. The box girder cracking was simulated approximately by removing the partial elements of the space-frame lattice model. Firstly, the partial elements at the regions of the bottom slab with larger principal tensile stresses were removed to analyze the stress state of the structure after bottom slab cracking; Secondly, the partial vertical elements at regions of the web with larger principal tensile stresses, which were caused by bottom slab cracking, were removed to simulate the stress state of the structure after web cracking.

Fig. 10. The space-frame lattice model of half bridge

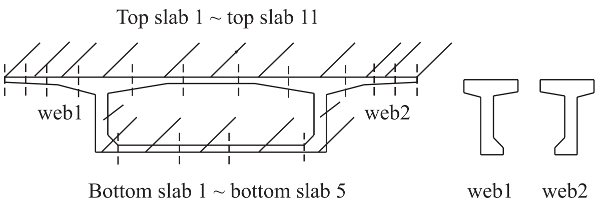

Fig. 11. The division of cross-section of box girder

4.3. Simulation of bottom slab cracking

The stresses at D (Fig. 2) were calculated and analyzed. The transverse elements of the bottom slab, with principal tensile stresses at D greater than 2.5 MPa, were then removed. With this, the transverse frame action of the bottom slab was interrupted and the redistribution of internal forces due to bottom slab cracking could be simulated. The location of bottom slab cracking is shown in Fig. 12a. The internal forces of the structure were redistributed after removal of partial elements of the bottom slab at cracked regions. The calculation results are the following.

4.3.1. Calculation results of normal stress under dead load after bottom slab cracking

Figs 13 and 14 show the data about variation of normal stress at A and C of the web under dead load along the half bridge after bottom slab cracking. In the following figures the σ is normal stress and the Δσ is variation of normal stress.

Above Figs shows that the increment of normal stress in the lower flange of web (point C) at cracking region is big after bottom slab cracking.

4.3.2. Calculation results of shear stress under dead load after bottom slab cracking

Fig. 15 shows the data about variation of shear stress of the web under dead load along the half bridge after bottom slab cracking. The shear stress at A, B and C in webs is regarded as the same approximate. In the following figures the τ is shear stress and the Δτ is variation of shear stress.

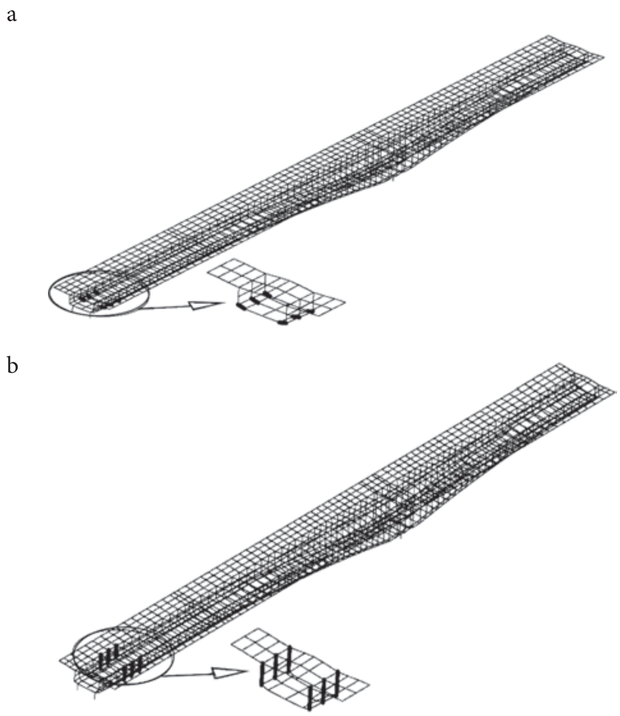

Fig. 12. The crack location of box girder: a – the location of bottom slab cracking; b – the location of web cracking

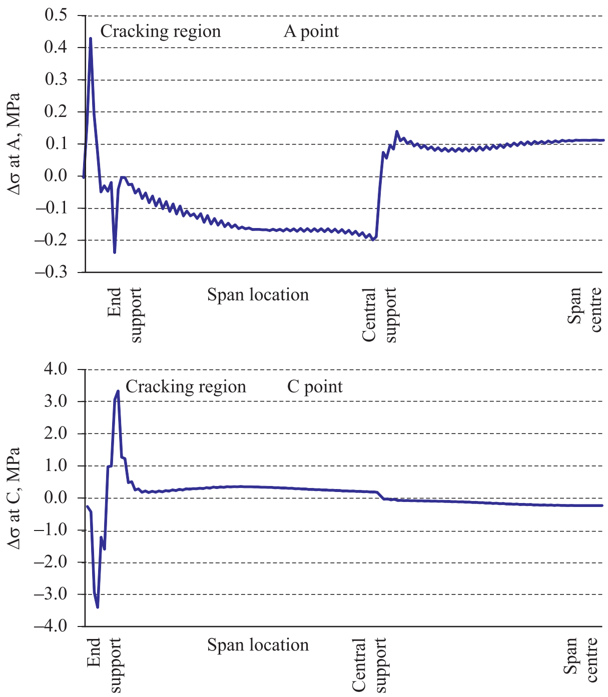

Fig. 13. Variation of normal stress of web under dead load after bottom slab cracking

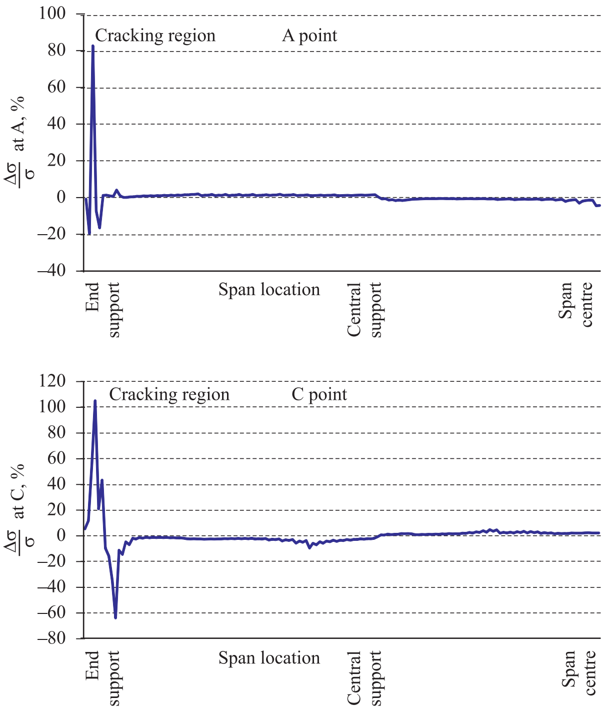

Fig. 14. $\frac{\Delta\sigma}{\sigma}$ of web under dead load after bottom slab cracking

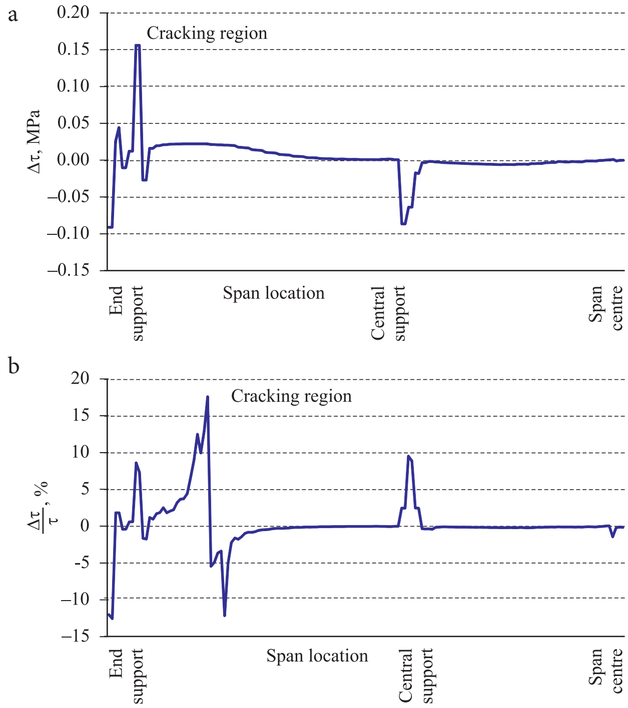

Fig. 15. Shear stress of web: a – $\Delta\tau$ of web after bottom slab cracking; b – $\frac{\Delta\tau}{\tau}$ of web after bottom slab cracking

It is obvious that the shear stress of web at cracking region increases greatly after bottom slab cracking.

4.3.3. Calculation results of deflection under dead load after bottom slab cracking

Fig. 16 shows the deflection variations of the box girder under dead load along the half bridge after bottom slab cracking.

It is apparent that the variation of box girder deflection under dead load after bottom slab cracking is the following: 1) the box girder at the side-span had downward variation of deflection, the max of which was about 4.7 cm; 2) the box girder at mid-span had upward variation of deflection, the max of which was about 6.8 cm.

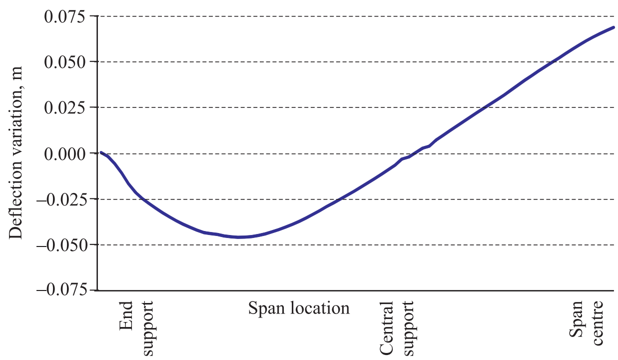

Fig. 16. The deflection variation of box girder after bottom slab cracking

4.3.4. Calculation results under live load after bottom slab cracking

The following results are concluded according to the calculation results:

1) The variation of normal stress in the lower flange of web at cracking region under live load is bigger, and the $\Delta\sigma$ and $\frac{\Delta\sigma}{\sigma}$ of which reach 1.7 MPa and 250%.

2) The variation of shear stress in web under live load is less, and the max $\Delta\tau$ and $\frac{\Delta\tau}{\tau}$ of which is 0.1 MPa and 26%.

3) The bottom slab cracking has less influence on the deflection of structure under live load, and the max increment is 0.8 mm.

4.3.5. Calculation results of principal tensile stress after bottom slab cracking

Fig. 17 shows the variation of max principal tensile stresses at A and C of the web along the half bridge after bottom slab cracking. The effects of dead load, live load, temperature and settlement of supports are taken into account and combined in the results of calculation.

Fig. 17 shows that the increment of principle tensile stress at C reaches 3.7 MPa after bottom slab cracking. Thus, the bottom slab cracking has great influence on the principle stress of web and it accelerates the incline cracking of web.

4.3.6. Brief summary

a) The removal of partial elements of the bottom slab at cracked regions generates the increase of local principal tensile stresses of the web.

b) Apart from the cracking region of the bottom slab the principal stress of the web is basically unchanged.

c) The cracking has a significant influence on the deflection of the structure, i.e., local cracking generates a change in deflection along the whole bridge.

d) The variation of structural deflection after bottom slab cracking is small under live load.

4.4. Simulation of web cracking

The principal tensile stress of the web near the cracked region of the bottom slab will increase and that may cause web cracking. On the basis of the simulation of bottom slab cracking the web cracking was simulated again by removing the vertical elements that connected the top slab and bottom slab at regions with more than principal tensile stress 2.5 MPa of the web. The cracked location of the web is shown in Fig. 12b.

Fig. 18 shows the variation of box girder deflection along the whole bridge when the web cracking happened due to cracking of the bottom slab.

Thus, the box girder deflection under dead load develops sequentially after web cracking, i.e., the box girder deflection at the side-span develops sequentially downward, while at mid-span develops sequentially upward. The max deflection at the side span is about 5.8 cm, while at mid-span is about 7.5 cm.

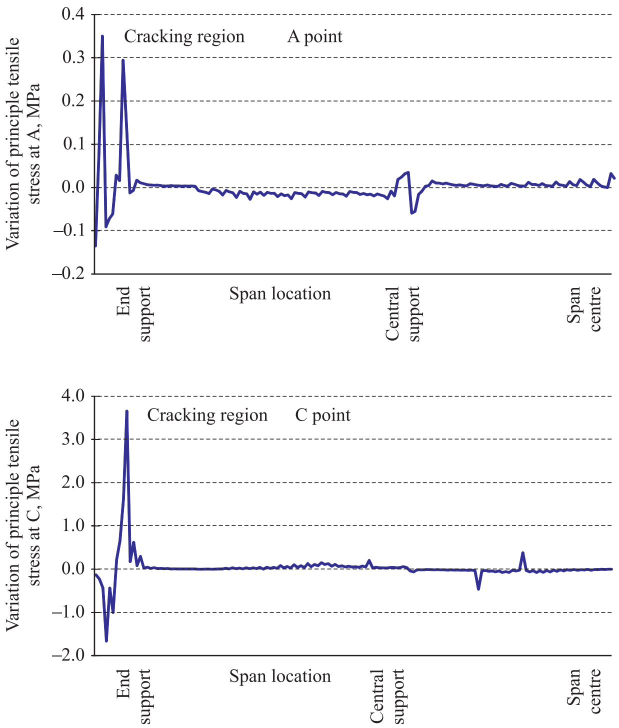

Fig. 17. The variation of max principal tensile stress of web after bottom slab cracking

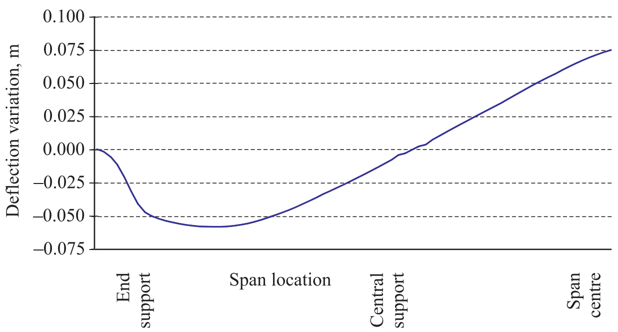

Fig. 18. The variation of deflection of box girder under dead load after cracking of web

4.5. Comparison

The calculation results are compared with the actual bridge status:

(1) The region with larger principal tensile stresses existed in the web of the side-span, i.e., the inclined cracking of the web was penetrative. This meets the first item of the inspecting results cited in Table 1.

(2) The cracks paralleled to the longitudinal prestressed tendons at regions with larger tensile stress outside the plane of the bottom slab of the box girder were produced mainly by the longitudinal prestressing in the bottom slab. Because these cracks were caused by bending they were local and not penetrative. This meets the second item of the inspecting results cited in Table 1.

(3) Although the whole process of box girder cracking and long-term deflection simulated by removing elements of the space-frame lattice model was approximate the calculation results meet the trend of the third item of the inspecting results cited in Table 1.

5. Conclusions

1. The crack has great influence on the deflection of structures according to the application of the space-frame lattice model in calculation and analysis of an actual bridge. An assessment for the process of cracking and deflection of bridges is as following:

First, the phenomenon of concrete cracking happens.

Second, the integral rigidity of the box girder cross-section is weakened due to cracking.

Third, the deflection of structure begins to develop because the effect of longitudinal prestressing in the bottom slab cannot be transferred to the whole cross-section of the box girder effectively.

Finally, the cracking and weakened rigidity of structure soften its members. Under external influences such as creep, temperature, live load etc, new cracking will appear and make the structure more flexible. Thus, cracking will occur continuously and the deflection will increase continuously.

2. Certainly, many aspects of the calculation model should be researched further in order to completely

simulate the whole process of long-term deflection of box girder bridges and to get more accurate results. At the same time, there is still need to accumulate more data about cracking and deflection of bridges to explain the reason of distress of bridges.

References

Barr, P. J; Angomas, F. 2010. Differences between Calculated and Measured Long-Term Deflections in a Prestressed Concrete Girder Bridge, *Journal of Performance of Constructed Facilities* 24(6): 603–609. http://dx.doi.org/10.1061/(ASCE)CF.1943-5509.0000121

Burgoyne, C.; Scantlebury, R. 2006. Why did Palau Bridge Collapse? *The Structural Engineer* 84(11): 30–37.

Du, G. H. 1994. *Analysis of Bridge Structure*. Shanghai: Tongji University Press. 236 p. ISBN 7560812856.

Grigorjeva, T.; Juozapaitis, A.; Kamaitis, Z.; Paeglitis, A. 2008. Finite Element Modelling for Static Behaviour Analysis of Suspension Bridges with Varying Rigidity of Main Cables, *The Baltic Journal of Road and Bridge Engineering* 3(3): 121–128. http://dx.doi.org/10.3846/1822-427X.2008.3.121-128

Gwoździewicz, P.; Jurkiewiez, B.; Destrebecq, J. F. 2000. Long Term Serviceability of Concrete Structures with Regards to Material Behaviors and Cyclic Loading, in *Proc. of the of Structures Congress 2000*. Philadelphia Pennsylvania USA: ASCE, 2000: 1–8. http://dx.doi.org/10.1061/40492(2000)159

Hu, D. 2005. Intelligent Control on Long-run Deflection for Prestressed Concrete Bridges, in The *2nd International Conference on Structural Health Monitoring of Intelligent Infrastructure.* November 16–18, 2005, Shenzhen, P. R. of China. 1563–1569.

Huang, H. D.; Xiang, Z. F.; Zheng, J. L. 2009. Analysis of Differential Shrinkage Deflection for PC Box-Girder Bridges, *Journal of Civil, Architectural and Environmental Engineering* 31(4): 60–65.

Kaklauskas, G.; Girdžius, R.; Bačinskas, D.; Sokolov, A. 2008. Numerical Deformation Analysis of Bridge Concrete Girders, *The Baltic Journal of Road and Bridge Engineering* 3(2): 51–56. http://dx.doi.org/10.3846/1822-427X.2008.3.51-56

Keogh, D. L.; O'Brien, E. J. 1996. Recommendation on the Use of a 3-D Grillage Model for Bridge Deck Analysis, *Structural Engineering Review* 8(4): 357–366. http://dx.doi.org/10.1016/0952-5807(95)00075-5

Krístek, V.; Bazant, Z. P.; Zich, M.; Kohoutková, A. 2006. Box Girder Bridge Deflections, *ACI Concrete International* 28(1): 55–63.

Krístek, V.; Kohoutková, A. 2006. Excessive Deflections of Concrete Bridges Affect Safety, Maintenance and Management, in *The 3rd International Conference on Bridge Maintenance, Safety and Management.* July 16–19, 2006, Porto. 355–356.

Lou, Z. H. 2006. Main Faults in Large Span Beam Bridges, *Journal of Highway and Transportation Research and Development* 23(4): 84–87. ISSN:1002-0268.0.2006-04-020

Liu, C.; Xu, D; Chen, A. R. 2009. Cause Analysis for Shear Crack and Deflection of Long Span Prestressed Concrete Box-Girder Bridge, *Journal of Tongji University* 37(1): 1–5.

Liu, C.; Xu, D. 2010. Space Frame Lattice Model for Stress Analysis of Bridge, *The Baltic Journal of Road and Bridge Engineering* 5(2): 98–103. http://dx.doi.org/10.3846/bjrbe.2010.14

O'Brien, E. J.; Keogh, D. L. 1998. Upstand Finite Element Analysis of Slab Bridges, *Computers and Structures* 69(6): 671–683. http://dx.doi.org/10.1016/S0045-7949(98)00148-5

O'Brien, E. J.; Keogh, D. L. 1999. *Bridge Deck Analysis.* 1st edition. Spon Press. 336 p. ISBN 0419225005. http://dx.doi.org/10.1016/S0045-7949(98)00148-5

Qi, D. C.; Zhang, Y, S; Li, Q. 2007. Reason Analysis and Countermeasures for Excessive Deflection of Midspan in Long-Span Continuous Rigid Frame Bridges, *Journal of Chongqing Jiaotong University* 26(6): 46–49.

Rodriguez, S. 2004. Design of Long Span Concrete Box Girder Bridges: Challenges and Solutions, in *Proc. of Structures Congress 2004 "Building on the Past: Securing the Future"*. Nashville TN USA: ASCE, 2004: 361–371.

Robertson, I. N. 2005. Prediction of Vertical Deflections for a Long-Span Prestressed Concrete Bridge Structure, *Engineering Structures* 27(12): 1820–1827. http://dx.doi.org/10.1016/j.engstruct.2005.05.013

Shao, F; Pan, D.; Li, F.; Liu, Y. 2011. Effects Analysis of Web Cracks on Long-Term Deformation of Large Span Pre-Stressed Concrete Continuous Box Girder Bridge, *Advanced Materials Research* (163–167): 1207–1212. http://dx.doi.org/10.4028/www.scientific.net/AMR.163-167.1207

Števula, M.; Vitek, J. L. 1998. Some Details of Long-Term Analysis of Concrete Bridges, in *The 2nd International PhD Symposium in Civil Engineering*. Budapest, Hungary. 26–28.

Xiang, H. 2001. *Theory of Advanced Bridge Structure.* Beijing: China Communications Press. 315 p. ISBN 7114037961.

Xie, J.; Wang, G. L.; Zheng, X. H. 2007. State of Art of Long-Term Deflection for Long Span Prestressed Concrete Box-Girder Bridge, *Journal of Highway and Transportation Research and Development* 24(1): 47–50.

Xu, D. 2008. *External Prestressing Technology of Bridge.* Beijing: China Communications Press. 333 p. ISBN 9787114073540.

Zhang, F. 2007. *Study of Some Key Points of Externally Prestressed Concrete Bridge in Elastic Stage.* Master's Thesis. Tongji University. Shanghai. 118 p.

Zheng, H. B.; Yu, X.; Hu, J.; Yan, Q. 2011. Parameter Sensitivity Analysis of Vertical Deflection for Long-Span Continuous Rigid-Frame Bridge, *Advanced Materials Research* (163–167): 1500–1504. http://dx.doi.org/10.4028/www.scientific.net/AMR.163-167.1500

Received 18 August 2010; accepted 6 April 2011